

# Numerical modelling of CO<sub>2</sub>-water-basalt interaction

A. P. GYSI\* AND A. STEFÁNSSON

Institute of Earth Sciences, University of Iceland, Sturlugata 7, 101 Reykjavik, Iceland

## ABSTRACT

The effects of CO<sub>2</sub> on water-basaltic glass interaction have been simulated at 25°C. The calculations indicate that addition of CO<sub>2</sub> (2–30 bar) to water significantly changes the reaction path. Initially, the pH is buffered between 4 and 6 by CO<sub>2</sub> ionization, with dissolution of basaltic glass and the formation of secondary minerals with SiO<sub>2</sub>, Mg-Fe carbonates and dolomite predominating. Upon the dissolution of additional basaltic glass and mineral fixation of CO<sub>2</sub>, the pH increases to >8 and (Ca)-Fe-Mg smectites, SiO<sub>2</sub>, Ca-Na zeolites and calcite become the dominant secondary minerals forming. The overall reaction path depends on the initial water composition, reactive surface area, and the composition of the phyllosilicates and carbonates forming. The key factors are the mobility of Mg<sup>2+</sup>, Fe<sup>2+</sup> and Ca<sup>2+</sup> and the competing reactions for these solutes among secondary minerals.

## Introduction

GLOBAL warming in recent decades is considered to result from increased atmospheric CO<sub>2</sub> levels due to the burning of fossil fuels. CO<sub>2</sub> sequestration into secondary minerals is considered one of the possible ways of reducing the level of atmospheric CO<sub>2</sub>. A project in SW Iceland, including scientists from different fields, is aiming to inject CO<sub>2</sub>-loaded waters from the Hellisheidi geothermal power plant into basaltic rock formations. Basalts are reactive and contain Ca, Mg and Fe to mineralize CO<sub>2</sub> into carbonates. Therefore, they are ideal for CO<sub>2</sub>-water-rock interaction.

Studies of natural analogues on water-basalt interaction at low CO<sub>2</sub> concentrations have shown quartz/chalcedony, clays and zeolites as well as calcite to be the dominant secondary minerals (Neuhoff *et al.*, 1999) whereas at elevated CO<sub>2</sub> concentrations, quartz and Fe<sup>2+</sup>, Mg- and Ca-carbonates dominate (Rogers *et al.*, 2006). However, the effect of CO<sub>2</sub> concentration on the reaction path during water-basalt interaction and the resulting water chemistry and mineralogical composition is somewhat unclear. Therefore, the

purpose of this work was to give insights into the effects of CO<sub>2</sub> on water-basalt interaction using geochemical modelling.

## Methods

Reaction-path calculations were carried out using the PHREEQC program, version 2.14.2 (Parkhurst and Appelo, 1999). The thermodynamic database for aqueous species, gas solubility and mineral reactions was updated for the present work. The approach adopted was to select the Gibbs free energy of formation for key aqueous species and minerals and to calculate the solubility constants for the mineral dissolution/precipitation reactions of interest from those data. The key aqueous species (base species) in the data set at present include H<sub>2</sub>O, H<sup>+</sup>, Na<sup>+</sup>, K<sup>+</sup>, Mg<sup>2+</sup>, Ca<sup>2+</sup>, Al<sup>3+</sup>, Fe<sup>2+</sup>, Fe<sup>3+</sup>, H<sub>4</sub>SiO<sub>4</sub>(aq), Ti(OH)<sub>4</sub>(aq), SO<sub>4</sub><sup>2-</sup>, HCO<sub>3</sub><sup>-</sup>, Cl<sup>-</sup> and F<sup>-</sup> selected from Cox *et al.* (1989), Hill (1990), Parker and Khodakovskii (1995), Gunnarsson and Arnórsson (2000), Benzeth *et al.* (2001), Palmer *et al.* (2001) and Stefánsson (2001). The thermodynamic properties for minerals were selected from the data set of Holland and Powell (1998) when available. Other values were selected from Stefánsson and Gíslason (2001), Neuhoff (2000) and Majzlan *et al.* (2004).

\* E-mail: apg2@hi.is

DOI: 10.1180/minmag.2008.072.1.55

The thermodynamic properties for phyllosilicates and carbonate solid solutions were calculated using the approach of Tardy and Fritz (1981) assuming ideal solid solution behaviour and taking into account appropriate elemental substitutions in common crystallographic sites in the case of phyllosilicates. The thermodynamic properties of the end-member phyllosilicates were taken from Tardy and Fritz (1981) and Holland and Powell (1998).

Calculations were carried out on CO<sub>2</sub>-water and basaltic glass from Stapafell, SW Iceland (Oelkers and Gíslason, 2001). Basaltic glass dissolution kinetics were included using the far-from-equilibrium rate expression of Gíslason and Oelkers (2003), assuming a geometric surface area of 250 cm<sup>2</sup> g<sup>-1</sup> and taking the saturation state of the primary phase to be that of an amorphous gel consisting of amorphous Al-hydroxide and amorphous silica (e.g. Oelkers and Gíslason, 2001).

Two sets of calculations were made at 25°C. In the first set, 10 g of basaltic glass was dissolved in 1000 ml of natural water (Langjökull, Laxá in Kjós), both closed and open to atmospheric CO<sub>2</sub>, in order to model natural water–basalt interaction. In the second set of calculations, 100 g of basaltic glass was allowed to dissolve in 1000 ml of water (HN-1) at initial CO<sub>2</sub> saturations of 2–30 bar in order to model the effects of CO<sub>2</sub> on the reaction path of water–basalt interaction. The HN-1 solution represents a mixture of geothermal and cold groundwater at Hellisheidi SW Iceland, and the Langjökull, and Laxá in Kjós solutions represent unpolluted rain water in Iceland and typical river water composition, respectively (Table 1).

## Results and discussion

### Low CO<sub>2</sub> systems

Figure 1 shows the pH evolution for progressive water–basalt interaction initially saturated with atmospheric CO<sub>2</sub>. The pH of Langjökull water rises rapidly to >9 and is more sensitive than water from Laxá in Kjós which has greater initial alkalinity. Systems open to atmospheric CO<sub>2</sub> reach a steady state at pH 7–8.5. Figure 2 shows the mineral sequence. At low reaction progress Al- and Fe-hydroxides are formed. With increasing basaltic glass dissolution, allophane, imogolite and/or kaolinite precipitate as well as smectites, and eventually chalcedony, Ca-zeolites and calcite are formed. These observations are

TABLE 1. Water compositions used in the simulations: Langjökull precipitation (S. R. Gíslason, pers. comm.); Laxá in Kjós river water (Stefánsson and Gíslason, 2001); HN-1 well water (Reykjavík Energy database, Iceland).

	Langjökull ( $\mu\text{mol/kg}$ )	Laxá in Kjós ( $\text{mmol/kg}$ )	HN-1 ( $\text{mmol/kg}$ )
<sup>a</sup> pH/°C	5.30/25	7.69/25	8.58/25
Si	0.001	0.148	2.11
Na	3.1	0.226	1.57
K	0.45	0.0074	0.031
Ca	0.15	0.088	0.18
Mg	0.35	0.067	0.33
S	0.35	0.022	0.083
Cl	3.15	0.256	0.25
F	5.029	0.0014	0.015
Fe	0.013	0.0025	0.00045
Al	0.054	0.0011	0.00085
<sup>b</sup> CO <sub>2</sub>	11.72	0.254	2.019

<sup>a</sup> pH calculated at 25°C

<sup>b</sup> saturated with atmospheric CO<sub>2</sub>

consistent with mineral assemblages observed in low-temperature basalt alteration systems (e.g. Neuhoﬀ *et al.*, 1999).

### Elevated CO<sub>2</sub> systems

Figure 3 shows the results of CO<sub>2</sub>–water–basaltic glass interaction initially saturated at 2, 10 and 30 bar CO<sub>2</sub>. At 2 bar, the basaltic glass

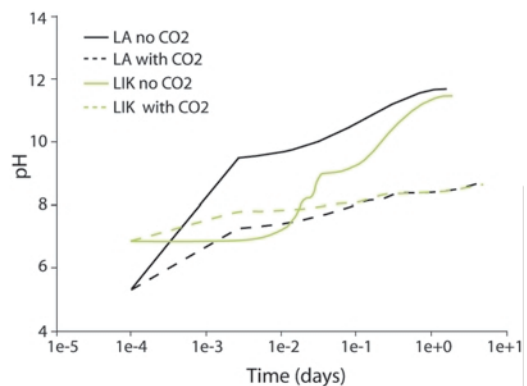


FIG. 1. pH changes during water–basaltic glass interaction as a function of time and water composition open to atmospheric CO<sub>2</sub> (surface water) and closed to atmospheric CO<sub>2</sub> (groundwater). LA = Langjökull; LIK = Laxá in Kjós.

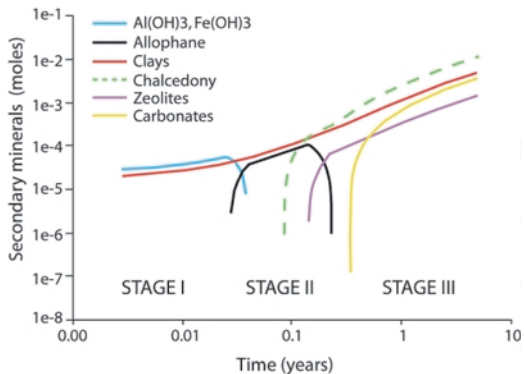


FIG. 2. Amount of secondary minerals formed during progressive water-basaltic glass interaction in contact with atmospheric CO<sub>2</sub>. Initial water composition is that of Langjökull.

reacts in ~4 y forming Si-Al minerals, Fe(II)-Mg-Ca carbonates, mixed clays, SiO<sub>2</sub> and finally zeolites. At 10 and 30 bar, the time for basaltic glass to react is ~35 y and the mineralogical sequence is similar to the initial stages for the 2 bar system.

The basaltic-glass dissolution rate depends on pH decreases and reaching a minimum at pH of ~6–7 (at 25°C) and increasing again with increasing pH (e.g. Gíslason and Oelkers, 2003). For the CO<sub>2</sub>-water-basaltic glass system, the pH was found to increase rapidly to 5–6, i.e. at minimum dissolution rate, whereas it became buffered by the ionization of CO<sub>2</sub>, dissolution of basaltic glass and precipitation of secondary minerals. At 2 bar CO<sub>2</sub>, the system pH increased to >7 when most of the initial CO<sub>2</sub> had been mineralized. However, at 10 and 30 bars CO<sub>2</sub>, the pH never reaches values >7 and the system was found to be locked at the minimum dissolution rate taking 10 times longer to dissolve all the basaltic glass.

#### Reaction path

In Fig. 4 we can see the reaction path of basaltic glass in contact with water saturated initially with 2 bar CO<sub>2</sub>. At low pH (5–7), the secondary minerals formed were carbonates (Fe-Mg carbonates and dolomite), Si-Al phases (allophane, imogolite and kaolinite) and SiO<sub>2</sub> (chalcedony) and the pH was buffered by CO<sub>2</sub> ionization, dissolution of basaltic glass and precipitation of secondary minerals. The amount of clay mineral

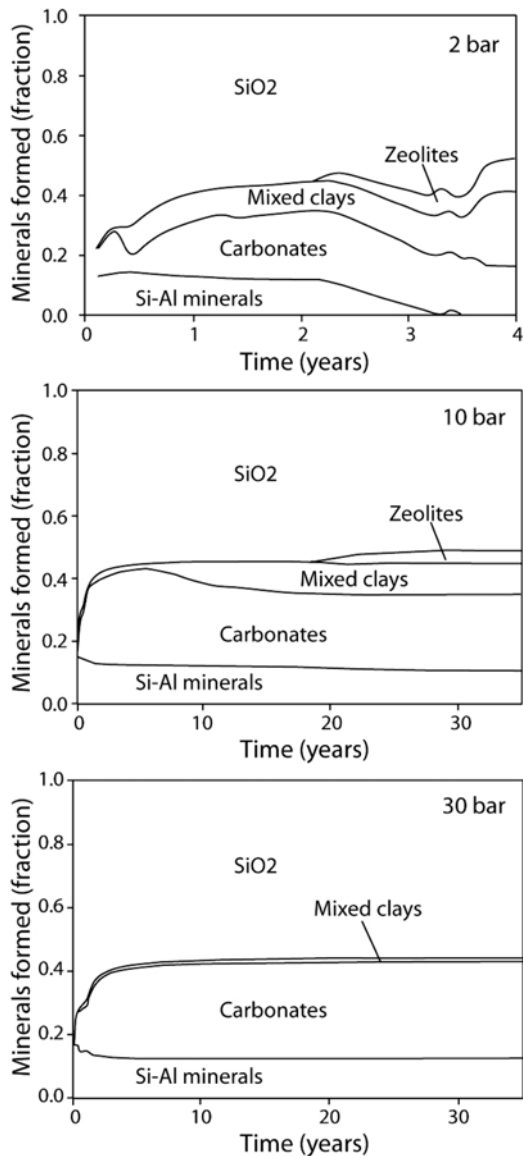


FIG. 3. Mole fraction of secondary minerals formed as a function of reaction progress for HN-1 water in contact with basaltic glass saturated with 2, 10 and 30 bars CO<sub>2</sub>. Mixed clays: celadonite, Ca-Fe-Mg smectites, Fe-Mg smectites and chlorite. Carbonates: calcite, dolomite, siderite, magnesite and Mg-Fe carbonate. Si-Al minerals: allophane, imogolite and kaolinite.

precipitation was insignificant at low reaction progress and the mobility of Ca, Mg and Fe was determined by the formation of carbonates reducing the aqueous CO<sub>2</sub> concentrations and

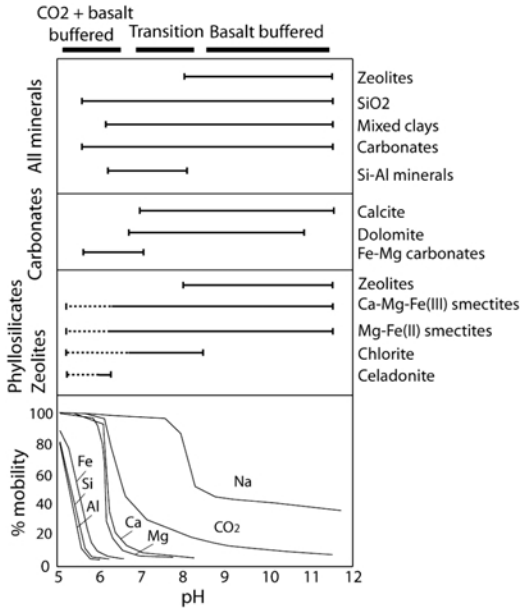


FIG. 4. Reaction-path diagram of HN-1 water in contact with basaltic glass and saturated at  $P_{CO_2} = 2$  bar. For % mobility see Stefánsson and Gíslason (2001).

increasing the pH of the system (Fig. 4). The turnover was reached when most of the CO<sub>2</sub> was fixed in the precipitated carbonates and the pH increased to >8. Under these conditions, the pH was buffered by basaltic glass dissolution and secondary mineral precipitation-dissolution reactions. The mobility of Mg and Fe were limited by the formation of smectites inhibiting the formation of Mg-Fe carbonates.

## Conclusions

In this study we presented the results of reaction-path simulation of CO<sub>2</sub>-water-basaltic glass at 0–30 bar CO<sub>2</sub>. Addition of CO<sub>2</sub> to the system was found to alter the reaction path. At low CO<sub>2</sub> concentrations the dissolution of basaltic glass resulted in an increase of the pH and formations of Fe(OH)<sub>3</sub>, Al(OH)<sub>3</sub>, Si-Al phases and clays. At elevated CO<sub>2</sub> concentrations, however, the pH was buffered at 5–6 and Fe-Mg carbonates, and dolomite precipitated as well as SiO<sub>2</sub>. Moreover, the simulation results gave an insight into the mobility of solutes and pH during progressive interaction of basaltic glass with CO<sub>2</sub>-water and its effect on mineralogical changes.

## Acknowledgements

This study was funded by the European Union through the MIN-GRO Research and Training Network (contract number: MRTN-CT-2006-035488) and by the Science Institute, University of Iceland.

## References

- Benezeth, P., Palmer, D.A. and Wesolowski, D.J. (2001) Aqueous high-temperature solubility studies. II. The solubility of boehmite at 0.03 m ionic strength as a function of temperature and pH as determined by in situ measurements. *Geochimica et Cosmochimica Acta*, **65**, 2097–2111.
- Cox, J.D., Wagman, D.D. and Medvedev, V.A. (1989) *CODATA Key Values for Thermodynamics*. Hemisphere Publishing Corp., New York.
- Gíslason, S.R. and Oelkers, E.H. (2003) Mechanism, rates, and consequences of basaltic glass dissolution: II. An experimental study of the dissolution rates of basaltic glass as a function of pH and temperature. *Geochimica et Cosmochimica Acta*, **67**, 3817–3832.
- Gunnarsson, I. and Arnorsson, S. (2000) Amorphous silica solubility and the thermodynamic properties of H<sub>4</sub>SiO<sub>4</sub> degrees in the range of 0 degrees to 350 degrees C at P-sat. *Geochimica et Cosmochimica Acta*, **64**, 2295–2307.
- Hill, P.G. (1990) A unified fundamental equation for the thermodynamic properties of H<sub>2</sub>O. *Journal of Physical and Chemical Reference Data*, **19**, 1233–1274.
- Holland, T.J.B. and Powell, R. (1998) An internally consistent thermodynamic data set for phases of petrological interest. *Journal of Metamorphic Geology*, **16**, 309–343.
- Majzlan, J., Navrotsky, A. and Schwertmann, U. (2004) Thermodynamics of iron oxides: Part III. Enthalpies of formation and stability of ferrihydrite (similar to Fe(OH)(3)), schwertmannite (similar to FeO(OH)(3/4)(SO4)(1/8)), and epsilon-Fe<sub>2</sub>O<sub>3</sub>. *Geochimica et Cosmochimica Acta*, **68**, 1049–1059.
- Neuhoff, P.S. (2000) *Thermodynamic properties and parageneses of rock-forming zeolites*. PhD thesis, Stanford University, Stanford, CA, USA.
- Neuhoff, P.S., Fridriksson, T., Arnorsson, S. and Bird, D.K. (1999) Porosity evolution and mineral paragenesis during low-grade metamorphism of basaltic lavas at Teigarhorn, eastern Iceland. *American Journal of Science*, **299**, 467–501.
- Oelkers, E.H. and Gíslason, S.R. (2001) The mechanism, rates and consequences of basaltic glass dissolution: I. An experimental study of the dissolution rates of basaltic glass as a function of aqueous Al, Si and oxalic acid concentration at 25

- degrees C and pH=3 and 11. *Geochimica et Cosmochimica Acta*, **65**, 3671–3681.
- Palmer, D.A., Benezeth, P. and Wesolowski, D.J. (2001) Aqueous high-temperature solubility studies. I. The solubility of boehmite as functions of ionic strength (to 5 molal, NaCl), temperature (100–290 degrees C), and pH as determined by in situ measurements. *Geochimica et Cosmochimica Acta*, **65**, 2081–2095.
- Parker, V.B. and Khodakovskii, I.L. (1995) Thermodynamic properties of the aqueous ions (2+ and 3+) of iron and the key compounds of iron. *Journal of Physical and Chemical Reference Data*, **24**, 1699–1745.
- Parkhurst, D.L. and Appelo, C.A.J. (1999) *User's guide to PHREEQC (Version 2) – A computer program for speciation, batch-reaction, one-dimensional transport, and inverse geochemical calculations*. US Geological Survey Water-Resources Investigations Report 99-4259: 310.
- Rogers, K.L., Neuhoff, P.S., Pedersen, A.K. and Bird, D.K. (2006) CO<sub>2</sub> metasomatism in a basalt-hosted petroleum reservoir, Nuussuaq, West Greenland. *Lithos*, **92**, 55-82.
- Stefánsson, A. (2001) Dissolution of primary minerals of basalt in natural waters – I. Calculation of mineral solubilities from 0 degrees C to 350 degrees C. *Chemical Geology*, **172**, 225–250.
- Stefánsson, A. and Gislason, S.R. (2001) Chemical weathering of basalts, Southwest Iceland: Effect of rock crystallinity and secondary minerals on chemical fluxes to the ocean. *American Journal of Science*, **301**, 513–556.
- Tardy, Y. and Fritz, B. (1981) An ideal solid-solution model for calculating solubility of clay minerals. *Clay Minerals*, **16**, 361–373.